INTERFACE FOCUS

royalsocietypublishing.org/journal/rsfs

Research





Cite this article: Souto-Trinei FA, Brea RJ, Devaraj NK. 2023 Biomimetic construction of phospholipid membranes by direct aminolysis ligations. *Interface Focus* **13**: 20230019. https://doi.org/10.1098/rsfs.2023.0019

Received: 15 April 2023 Accepted: 19 May 2023

One contribution of 9 to a theme issue 'Cell mimicry: bottom-up engineering of life'.

Subject Areas:

chemical biology, nanotechnology, synthetic biology

Keywords:

phospholipid, self-assembly, artificial cell, aminolysis, synthetic biology

Authors for correspondence:

Roberto J. Brea

e-mail: roberto.brea@udc.es

Neal K. Devaraj

e-mail: ndevaraj@ucsd.edu

Electronic supplementary material is available online at https://doi.org/10.6084/m9.figshare. c.6673513.

THE ROYAL SOCIETY

Biomimetic construction of phospholipid membranes by direct aminolysis ligations

Federica A. Souto-Trinei¹, Roberto J. Brea¹ and Neal K. Devaraj²

(D) FAS-T, 0000-0003-1785-6078; RJB, 0000-0002-0321-0156; NKD, 0000-0002-8033-9973

Construction of artificial cells requires the development of straightforward methods for mimicking natural phospholipid membrane formation. Here we describe the use of direct aminolysis ligations to spontaneously generate biomimetic phospholipid membranes from water-soluble starting materials. Additionally, we explore the suitability of such biomimetic approaches for driving the *in situ* formation of native phospholipid membranes. Our studies suggest that non-enzymatic ligation reactions could have been important for the synthesis of phospholipid-like membranes during the origin of life, and might be harnessed as simplified methods to enable the generation of lipid compartments in artificial cells.

1. Background

The construction of artificial cells from purely synthetic components is an emerging area of bottom-up synthetic biology [1,2]. Artificial cells have the potential to shed light on numerous biological processes, as well as organize chemical reactions in specific compartments [3]. Therefore, there has been increasing interest in developing innovative strategies for the fabrication of synthetic cells. Chemoselective ligation chemistries have been demonstrated to be powerful tools for the convergent assembly of lipid fragments, providing straightforward methodologies for the construction of artificial phospholipid membranes [4]. One of the most efficient ligation strategies is native chemical ligation (NCL) [5,6]. While NCL is widely used for synthesizing large peptides and nucleic acids [7-9], this non-enzymatic and chemoselective approach has been also employed for rapidly preparing phospholipids in situ from watersoluble thioesters [10-13]. However, NCL is limited by the necessity for an N-terminal cysteine [5,6]. Therefore, cysteine-free ligation methodologies have also been developed for the synthesis of biomimetic phospholipids [14-18]. Rather than relying on N-terminal cysteines, we hypothesized that a simpler and straightforward method for phospholipid membrane generation could be built using direct aminolysis [19-23] as the key ligation reaction.

Direct aminolysis uses the inherent nucleophilicity of *N*-terminal amines for the construction of amide bonds via reaction with *N*-acyl donors, notably, C-terminal thioesters [20–24]. These ligations tend to be significantly slower than NCL [25]. Reaction rates can be greatly increased by the addition of appropriate catalysts, such as metal ions or imidazole. Metal ion-assisted aminolysis has proven to be an effective methodology for the formation of relevant biomolecules [26–28]. For instance, the coordination of silver ions to peptide thioesters facilitates the acyl migration to amino moieties, which is frequently used for the preparation of cyclic peptides [29]. Alternatively, imidazole-catalysed aminolysis has been employed to synthesize large and complex peptides [30–32]. The mechanism of the reaction likely involves the reaction of imidazole with the C-terminal thioester, affording an acyl imidazole intermediate that subsequently reacts with the amine-containing ligation partner to form the final

© 2023 The Authors. Published by the Royal Society under the terms of the Creative Commons Attribution License http://creativecommons.org/licenses/by/4.0/, which permits unrestricted use, provided the original author and source are credited.

¹Biomimetic Membrane Chemistry (BioMemChem) Group, CICA—Centro Interdisciplinar de Química e Bioloxía, Universidade da Coruña, Rúa As Carballeiras, 15701 A Coruña, Spain

²Department of Chemistry and Biochemistry, University of California, San Diego, 9500 Gilman Drive, La Jolla, CA 92093. USA

royalsocietypublishing.org/journal/rsfs Interface Focus 13: 20230019

Downloaded from https://royalsocietypublishing.org/ on 15 September 2023

amide linkage. Considering the importance of this ligation strategy, it would be exciting to develop a straightforward methodology based on direct aminolysis to rapidly prepare phospholipids from water-soluble precursors. Here we describe the use of metal- and imidazole-promoted reactions for the *in situ* generation of phospholipid vesicles via direct aminolysis between amine-containing lysophospholipids and fatty acyl thioesters (figure 1).

2. Methods

2.1. Chemicals and materials

Commercially available 1-palmitoyl-2-hydroxy-sn-glycero-3phosphocholine (Lyso C₁₆ PC) and 1-palmitoyl-2-oleoyl-sn-glycerol-3-phosphocholine (POPC) were used as obtained from Avanti Polar Lipids. β-Alanine (H₂N-β-Ala-OH), N,N'-diisopropylcarbodiimide (DIC), 4-dimethylaminopyridine (DMAP), trifluoroacetic acid (TFA), oleic acid, N-(3-dimethylaminopropyl)-N'-ethylcarbodiimide hydrochloride (EDC.HCl), N-acetyl (SNAC), sodium 2-mercaptoethanesulfonate (MESNA) [33,34], copper(II) bromide (CuBr₂), silver nitrate (AgNO₃), tetrakis(acetonitrile)copper(I) hexafluorophosphate (Cu(CH₃CN)₄PF₆), zinc iodide (ZnI₂), manganese(II) bromide (MnBr₂), nickel(II) iodide (NiI₂), gold(I) chloride (AuCl), gold(III) chloride (AuCl₃), silver(I) triflate (AgOTf), imidazole (Im), 1-methylimidazole (1-MeIm), 2-methylimidazole (2-MeIm), 4(5)methylimidazole (4(5)-MeIm), 2-ethylimidazole (2-EtIm), 2-undecylimidazole (2-^{Un}Im), 2-ethyl-4-methylimidazole (2-^{Et}-4-^{Me}Im), Boc-L-histidine (Boc-His-OH), histidine (H₂N-His-OH), histamine, 1,6-diphenyl-1,3,5-hexatriene (DPH) and 8-hydroxypyrene-1,3,6trisulfonic acid (HPTS) were obtained from Sigma-Aldrich. Texas Red 1,2-dihexadecanoyl-sn-glycero-3-phosphoethanolamine, triethylammonium salt (Texas Red DHPE) was obtained from Life Technologies. Deuterated chloroform (CDCl₃), methanol (CD₃OD) and DMSO (d₆-DMSO) were obtained from Cambridge Isotope Laboratories. All reagents obtained from commercial suppliers were used without further purification unless otherwise noted. Analytical thin-layer chromatography was performed on E. Merck silica gel 60 F254 plates. Compounds, which were not UV active, were visualized by dipping the plates in a ninhydrin or potassium permanganate solution and heating. Silica gel flash chromatography was performed using E. Merck silica gel (type 60SDS, 230-400 mesh). Solvent mixtures for chromatography are reported as v/v ratios. HPLC analysis was carried out on an Eclipse Plus C8 analytical column with Phase A/Phase B gradients [Phase A: H₂O with 0.1% formic acid; Phase B: MeOH with 0.1% formic acid]. HPLC purification was carried out on Zorbax SB-C18 semipreparative column with Phase A/Phase B gradients [Phase A: H₂O with 0.1% formic acid; Phase B: MeOH with 0.1% formic acid]. Proton nuclear magnetic resonance (¹H NMR) spectra were recorded on Varian VX-500 MHz or Jeol Delta ECA-500 MHz spectrometers and were referenced relative to residual proton resonances in CDCl₃ (at 7.24 ppm), CD₃OD (at 4.87 or 3.31 ppm) or d₆-DMSO (at 2.50 ppm). Chemical shifts were reported in parts per million (ppm, δ) relative to tetramethylsilane (δ 0.00). ¹H NMR splitting patterns are assigned as singlet (s), doublet (d), triplet (t), quartet (q) or pentuplet (p). All firstorder splitting patterns were designated based on the appearance of the multiplet. Splitting patterns that could not be readily interpreted are designated as multiplet (m) or broad (br). Carbon nuclear magnetic resonance (13C NMR) spectra were recorded on Varian VX-500 MHz or Jeol Delta ECA-500 MHz spectrometers and were referenced relative to residual proton resonances in CDCl₃ (at 77.23 ppm), CD₃OD (at 49.15 ppm) or d₆-DMSO (at 39.51 ppm). Electrospray ionization time of flight (ESI-TOF) spectra were obtained on an Agilent 6230 Accurate-Mass TOFMS mass spectrometer. Anisotropy measurements were obtained with a SPEX FluoroMax-3 spectrofluorometer. Transmission electron microscopy (TEM) images were recorded on an FEI TecnaiTM Sphera 200 kV microscope equipped with a LaB₆ electron gun, using the standard cryotransfer holders developed by Gatan, Inc.

2.2. Synthesis of lysophospholipids

Lysophospholipid 1 was synthesized according to electronic supplementary material, scheme S1.

2.2.1. *N*-Boc-β-Ala-OH (**4**)

To a solution of H₂N-β-Ala-OH (500.0 mg, 5.61 mmol) in H₂O (8.42 ml) were successively added Boc₂O (8.42 ml, 8.42 mmol, $1\,M$ solution in THF) and Et₃N (2.35 ml, 16.83 mmol). After $3\,h$ stirring at rt, the solution was acidified to pH 3 by the addition of HCl (10%), and extracted with CH_2Cl_2 (3 × 5 ml). The combined organic layers were dried (Na₂SO₄), filtered and concentrated, providing a yellow oil, which was purified by flash chromatography (0-3% MeOH in CH₂Cl₂), affording 928.0 mg of N-Boc- β -Ala-OH as a white solid (87%, R_f = 0.74 (70% MeOH in CH_2Cl_2)). ¹H NMR (CDCl₃, 500.13 MHz, δ): 6.28 (s, 0.3H, 0.3 × NH), 5.06 (s, 0.7H, 0.7 × NH), 3.40 (m, 2H, $1 \times CH_2$), 2.58 (m, 2H, $1 \times CH_2$), 1.44 (s, 9H, $3 \times CH_3$). ¹³C NMR (CDCl₃, 125.77 MHz, δ): 178.0 and 176.5, 157.8 and 156.1, 81.3 and 79.9, 37.3 and 36.0, 34.7, 28.6. MS (ESI-TOF) (m/z (%)): 212 ([M+Na]+, 100). HRMS (ESI-TOF) calculated for C₈H₁₅NO₄Na ([M + Na]⁺) 212.0893, found 212.0895.

2.2.2. 1-Palmitoyl-2-(*N*-Boc-β-Ala)-*sn*-glycero-3-phosphocholine (**5**)

A solution of N-Boc-β-Ala-OH (4, 61.1 mg, 322.6 μmol) in CH₂Cl₂ (15 ml) was stirred at rt for 10 min, and then DIC (93.8 μl, 604.8 μmol) and DMAP (24.6 mg, 201.6 μmol) were successively added. After 10 min stirring at rt, 1-palmitoyl-2hydroxy-sn-glycero-3-phosphocholine (50.0 mg, 100.8 μmol) was added. After 12 h stirring at rt, the solvent was removed under reduced pressure, and the crude was purified by HPLC, affording 52.2 mg of 5 as a colourless foam (78%, $t_R = 6.8$ min (Zorbax SB-C18 semipreparative column, 5% Phase A in Phase B, 15.5 min)). ¹H NMR (CDCl₃, 500.13 MHz, δ): 6.15 (br s, 1H, 0.3H, 0.3 \times NH), 5.41 (br s, 0.7H, 0.7 \times NH), 5.21 (m, 1H, 1 \times CH), 4.40-4.26 (m, 3H, $1.5 \times CH_2$), 4.17-4.08 (m, 1H, $0.5 \times CH_2$), 4.07-3.94 (m, 2H, $1 \times CH_2$), 3.85-3.75 (m, 2H, $1 \times CH_2$), 3.38-3-3.9431 (m, 2H, $1 \times CH_2$), 3.30 (s, 9H, $3 \times CH_3$), 2.59-2.46 (m, 2H, $1 \times CH_2$), 2.27 (t, J = 7.6 Hz, 2H, $1 \times CH_2$), 1.61–1.50 (m, 2H, $1 \times$ CH₂), 1.40 (s, 9H, $3 \times \text{CH}_3$), 1.30–1.20 (m, 24H, $12 \times \text{CH}_2$), 0.86 (t, I = 6.8 Hz, 3H, $1 \times \text{CH}_3$). ¹³C NMR (CDCl₃, 125.77 MHz, δ): 173.8, 171.8, 156.1, 79.4, 70.9, 66.3, 64.2, 62.6, 59.8, 54.5, 36.4, 34.9, 34.2, 32.1, 29.9, 29.9, 29.8, 29.7, 29.5, 29.5, 29.3, 28.6, 25.0, 22.9, 14.3. MS (ESI-TOF) $(m/z \ (\%))$: 689 $([M + Na]^+, 100)$. HRMS (ESI-TOF) calculated for $C_{32}H_{63}N_2O_{10}PNa$ ([M + Na]⁺) 689.4113, found 689.4114.

2.2.3. 1-Palmitoyl-2-(β -Ala)-sn-glycero-3-phosphocholine (**1**)

A solution of 1-palmitoyl-2-(N-Boc- β -Ala)-sn-glycerol-3-phosphocholine (5, 9.0 mg, 13.5 μmol) in 1 ml of TFA/CH₂Cl₂ (1:1) was stirred at rt for 15 min. After the removal of the solvent, the residue was dried under high vacuum for 3 h. Then, the corresponding residue was diluted in MeOH (500 μl), filtered using a 0.2 μm syringe-driven filter, and the crude solution was purified by HPLC, affording 7.2 mg of the lysophospholipid 1 as a colourless oil (80%, t_R = 8.6 min (Zorbax SB-C18 semipreparative column, 50% *Phase A* in *Phase B*, 5 min, and then 5% *Phase A* in *Phase B*, 10 min)). ¹H NMR (CD₃OD, 500.13 MHz, δ): 5.19 (m, 1H, 1 × CH), 4.37–4.32 (dd, 1H, J_1 = 3.9 Hz, J_2 = 12.1 Hz, 0.5 × CH₂), 4.26–4.16 (m, 3H, 1.5 × CH₂), 4.14–4.06 (m, 1H,

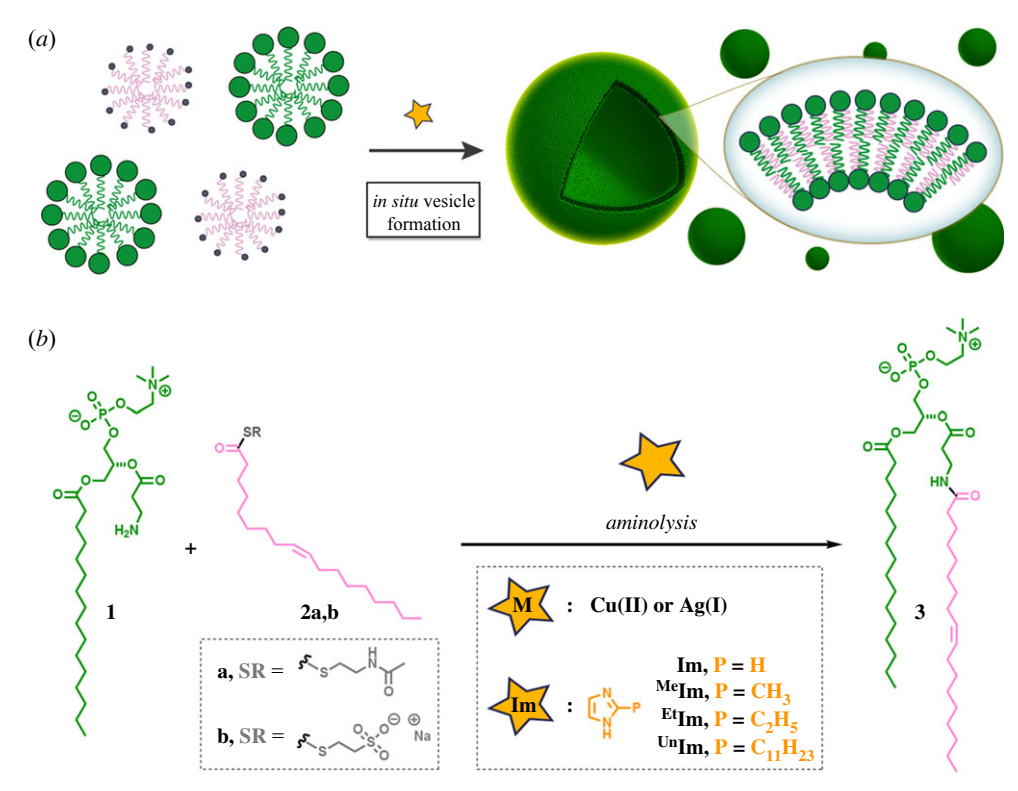


Figure 1. Biomimetic construction of phospholipid membranes based on direct aminolysis. (a) Schematic of spontaneous vesicle assembly induced by aminolysis-based amidophospholipid synthesis. (b) De novo formation of phospholipids (3) by metal- or imidazole-promoted aminolysis ligations between an amine-functionalized lysophospholipid (1) and an oleoyl thioester (2a,b).

 $0.5 \times \text{CH}_2$), 4.03-3.95 (m, 1H, $0.5 \times \text{CH}_2$), 3.61-3.56 (m, 2H, $1 \times \text{CH}_2$), 3.22-3.13 (m, 2H, $1 \times \text{CH}_2$), 3.17 (s, 9H, $3 \times \text{CH}_3$), 2.82-2.65 (m, 2H, $1 \times \text{CH}_2$), 2.28 (t, J=7.4 Hz, 2H, $1 \times \text{CH}_2$), 1.59-1.50 (m, 2H, $1 \times \text{CH}_2$), 1.30-1.20 (m, 24H, $12 \times \text{CH}_2$), 0.85 (t, J=6.8 Hz, 3H, $1 \times \text{CH}_3$). ^{13}C NMR (CD₃OD, 125.77 MHz, δ): 175.1, 171.5, 73.4, 67.5, 65.2, 63.3, 60.6, 54.8, 36.4, 34.9, 33.2, 32.8, 31.0, 31.0, 31.0, 31.0, 30.9, 30.9, 30.8, 30.7, 30.6, 30.4, 26.1, 23.9, 14.6. MS (ESI-TOF) (m/z (%)): 567 ([MH]⁺, 100). HRMS (ESI-TOF) calculated for $\text{C}_{27}\text{H}_{56}\text{N}_2\text{O}_8\text{P}}$ ([MH]]⁺) 567.3769, found 567.3770.

2.3. Synthesis of thioesters

Downloaded from https://royalsocietypublishing.org/ on 15 September 2023

Thioesters 2a and 2b were synthesized according to electronic supplementary material, schemes S2a and S2b, respectively.

2.3.1. SNAC oleoyl thioester (2a)

A solution of oleic acid (100.0 mg, 354.0 µmol) in CH₂Cl₂ (3.54 ml) was stirred at 0°C for 10 min, and then DMAP (4.3 mg, 35.4 μmol) and EDC.HCl (74.6 mg, 389.0 μmol) were successively added. After 10 min stirring at 0°C, SNAC (45.0 µl, 425.0 µmol) was added. After 5 h stirring at rt, the solvent was removed under reduced pressure, and the crude was purified by flash chromatography (10-50% EtOAc in hexanes), affording 131.1 mg of **2a** as a white solid (97%, $R_f = 0.28$ (50% EtOAc in hexanes)). 1 H NMR (CDCl₃, 500.13 MHz, δ): 6.08 (br s, 1H, 1 × NH), 5.35–5.23 (m, 2H, $2 \times CH$), 3.37 (q, J = 6.2 Hz, 2H, $1 \times CH$ CH₂), 2.97 (t, J = 6.5 Hz, 2H, $1 \times$ CH₂), 2.51 (t, J = 7.4 Hz, 2H, $1 \times CH_2$), 1.98–1.92 (m, 4H, $2 \times CH_2$), 1.92 (s, 3H, $1 \times CH_3$), 1.65-1.54 (m, 2H, $1 \times CH_2$), 1.32-1.16 (m, 20H, $10 \times CH_2$), 0.83(t, J = 6.8 Hz, 3H, $1 \times \text{CH}_3$). ¹³C NMR (CDCl₃, 125.77 MHz, δ): 200.2, 170.4, 130.1, 129.7, 44.2, 39.8, 32.0, 29.8, 29.7, 29.6, 29.4, 29.2, 29.1, 29.0, 28.5, 27.3, 27.2, 25.7, 23.3, 22.7, 14.2. MS (ESI-TOF) (m/z (%)): 406 $([M + Na]^+, 100)$. HRMS (ESI-TOF) calculated for C₂₂H₄₁NO₂SNa ([M + Na]⁺) 406.2750, found 406.2753.

2.3.2. MESNA oleoyl thioester (2b)

A solution of oleic acid (189.2 mg, 670.0 µmol) in CH₂Cl₂ (5 ml) was stirred at 0°C for 10 min, and then DMAP (7.4 mg, 60.9 µmol) and EDC.HCl (128.4 mg, 670.0 µmol) were successively added. After 10 min stirring at 0°C, MESNA (100.0 mg, 609.1 µmol) was added. After 5 h stirring at rt, the mixture was extracted with H₂O (2 × 3 ml) and the combined aqueous phases were washed with EtOAc (3 ml). After evaporation of H₂O under reduced pressure, the residue was washed with CH₃CN (5 ml) and then filtered to yield 194.7 mg of 2b [44] as a white solid (75%). 1 H NMR (d₆-DMSO, 500.13 MHz, δ): 5.36–5.27 (m, 2H, $2 \times CH$), 3.05-2.99 (m, 2H, $1 \times CH_2$), 2.60-2.51 (m, 4H, $2 \times CH_2$) CH₂), 2.02–1.92 (m, 4H, $2 \times \text{CH}_2$), 1.58–1.49 (m, 2H, $1 \times \text{CH}_2$), 1.34–1.18 (m, 20H, $10 \times \text{CH}_2$), 0.85 (t, J = 6.9 Hz, 3H, $1 \times \text{CH}_3$). ¹³C NMR (d₆-DMSO, 125.77 MHz, δ): 198.7, 129.8, 129.7, 51.0, 43.4, 31.4, 29.2, 29.1, 28.9, 28.8, 28.7, 28.6, 28.5, 28.3, 26.7, 26.6, 25.1, 24.4, 22.2, 14.1. MS (ESI-TOF) (m/z (%)): 429 ([MH]+, 100). HRMS (ESI-TOF) calculated for C₂₀H₃₈NaO₄S₂ ([MH]⁺) 429.2104, found 429.2105.

2.4. Synthesis of phospholipids

Phospholipids 3 and POPC were synthesized according to electronic supplementary material, schemes S3a and S3b, respectively.

2.4.1. Amidophospholipid 1-palmitoyl-2-[β-Ala-(oleoyl)]-*sn*-qlycero-3-phosphocholine (**3**)

1-Palmitoyl-2-(β-Ala)-sn-glycerol-3-phosphocholine (1, 7.0 mg, 10.5 μmol) was treated with a 30 mM solution of MESNA oleoyl thioester (2b, 4.5 mg, 10.5 μmol) in 1.5 M solution of imidazole in $\rm H_2O$ (351 μl), and the reaction was stirred and heated at 37°C. After 2 h, the mixture was diluted in MeOH (351 μl), filtered using a 0.2 μm syringe-driven filter, and the crude solution was purified by HPLC, affording 7.8 mg of the amidophospholipid 3 as a white solid (90%, $\rm t_R$ = 13.2 min (Zorbax SB-C18 semipreparative column, *Phase B*, 15.5 min)). $\rm ^1H$ NMR

(CDCl₃, 500.13 MHz, δ): 6.92–6.82 (m, 1H, 1 × NH), 5.36–5.26 (m, 2H, 2 × CH), 5.24–5.16 (m, 1H, 1 × CH), 4.48–4.24 (m, 3H, 1.5 × CH₂), 4.20–3.96 (m, 3H, 1.5 × CH₂), 3.90–3.72 (m, 2H, 1 × CH₂), 3.51–3.41 (m, 2H, 1 × CH₂), 3.30 (s, 9H, 3 × CH₃), 2.62–2.47 (m, 2H, 1 × CH₂), 2.27 (t, J = 7.9 Hz, 2H, 1 × CH₂), 2.14 (t, J = 7.5 Hz, 2H, 1 × CH₂), 2.00–1.92 (m, 4H, 2 × CH₂), 1.61–1.50 (m, 4H, 2 × CH₂), 1.33–1.17 (m, 44H, 22 × CH₂), 0.85 (t, J = 6.7 Hz, 6H, 2 × CH₃). 13 C NMR (CDCl₃, 125.77 MHz, δ): 174.0, 173.9, 171.8, 130.2, 129.9, 76.8, 71.0, 66.5, 64.5, 62.4, 59.9, 54.7, 51.1, 36.7, 35.3, 34.6, 34.2, 32.2, 32.1, 30.0, 30.0, 29.9, 29.9, 29.9, 29.8, 29.6, 29.6, 29.5, 29.4, 29.3, 27.4, 27.4, 26.0, 25.1, 22.9, 22.9, 14.4. MS (ESITOF) (m/z (%)): 853 ([M + Na]⁺, 100). HRMS (ESI-TOF) calculated for C₄₅H₈₇N₂O₉PNa ([M + Na]⁺) 853.6041, found 853.6042.

2.4.2. 1-Palmitoyl-2-oleoyl-sn-glycerol-3-phosphocholine

1-Palmitoyl-2-hydroxy-sn-glycero-3-phosphocholine (Lyso C_{16} PC, 5.2 mg, 10.5 µmol) was treated with a 30 mM solution of MESNA oleoyl thioester (2b, 4.5 mg, 10.5 μmol) in 1.5 M solution of imidazole in H₂O (351 µl), and the reaction was stirred and heated at 37°C. After 2 h, the mixture was diluted in MeOH (351 µl), filtered using a 0.2 µm syringe-driven filter, and the crude solution was purified by HPLC, affording 6.9 mg of the phospholipid **POPC** as a white solid (86%, $t_R = 14.1 \text{ min}$ (Zorbax SB-C18 semipreparative column, Phase B, 15.5 min)). ¹H NMR (CDCl₃, 500.13 MHz, δ): 5.36–5.25 (m, 2H, 2 × CH), 5.20-5.09 (m, 1H, $1 \times CH$), 4.40-4.30 (m, 1H, $0.5 \times CH_2$), 4.29-4.304.18 (m, 2H, $1 \times CH_2$), 4.12–4.04 (dd, $J_1 = 7.6 \text{ Hz}$, $J_2 = 4.6 \text{ Hz}$, 1H, $0.5 \times CH_2$), 3.99-3.80 (m, 2H, $1 \times CH_2$), 3.73-3.65 (m, 2H, $1 \times CH_2$) CH_2), 3.28 (s, 9H, 3× CH_3), 2.31–2.20 (m, 4H, 2× CH_2), 2.03– 1.91 (m, 4H, 2 × CH₂), 1.62-1.47 (m, 4H, 2 × CH₂), 1.36-1.14 (m, 44H, $22 \times \text{CH}_2$), 0.85 (t, J = 6.7 Hz, 6H, $2 \times \text{CH}_3$). ¹³C NMR (CDCl₃, 125.77 MHz, δ): 173.8, 173.4, 130.2, 129.9, 70.6, 66.4, 63.6, 63.1, 59.5, 54.5, 34.5, 34.3, 32.1, 32.1, 30.0, 30.0, 30.0, 30.0, 29.9, 29.9, 29.8, 29.8, 29.8, 29.7, 29.6, 29.6, 29.5, 29.5, 29.5, 29.4, 29.4, 29.4, 27.4, 25.2, 25.1, 22.9, 14.4. MS (ESI-TOF) (m/z (%)): 760 ($[M + H]^+$, 100). HRMS (ESI-TOF) calculated for $C_{42}H_{83}NO_8P$ $([M + H]^{+})$ 760.5851, found 760.5853.

2.5. Analysis of micelle size and critical micelle

concentrations

In total, 100 μ l of aqueous solutions (10 mM, 1 mM, 100 μ M, 10 μ M and 1 μ M) of **2b** or **Lyso** C₁₆ PC were analysed by dynamic light scattering (DLS) to determine the micelle sizes (electronic supplementary material, figure S2) and the critical micelle concentrations (CMCs) (electronic supplementary material, figure S3).

2.6. HPLC/ELSD/MS analysis

Phospholipid synthesis was performed in the appropriate conditions as described above. Aliquots of 1.5 μ l of phospholipid (3 or POPC) sample were taken at various time points, diluted with 50 μ l of MeOH and analysed using an Eclipse Plus C8 analytical column (5% *Phase A* in *Phase B*, 5.5 min) with an evaporative light scattering detector (ELSD) at a flow of 1.0 ml min⁻¹. For all LC/MS runs, solvent *Phase A* consisted of H₂O with 0.1% formic acid and solvent *Phase B* of MeOH with 0.1% formic acid.

2.7. Fluorescence microscopy of phospholipid membrane vesicles

2.7.1. Hydration method

In total, $10 \,\mu$ l of a 20 mM solution of phospholipid (3 or POPC) in CHCl₃ was added to a 1 ml vial, placed under N₂ and dried for 15 min to prepare a lipid film. Then, 200 μ l of H₂O was

added and the solution was tumbled at 25°C for 1 h. Afterwards, 0.1 μ l of a 100 μ M Texas Red DPHE dye solution in EtOH was added to 10 μ l of this 1 mM aqueous solution of phospholipid (3 or **POPC**) and the mixture was briefly agitated. The corresponding mixture was finally monitored by fluorescence and phase contrast microscopy to determine the vesicle structure.

2.7.2. Sonication method

In total, 10 µl of a 20 mM solution of phospholipid (3 or POPC) in CHCl $_3$ was added to a 1 ml vial, placed under N_2 and dried for 15 min to prepare a lipid film. Then, 200 µl of H_2O was added, and the resulting mixture was sonicated with heat ($\approx55^{\circ}C$) for 1 h. Afterwards, 0.1 µl of a 100 µM Texas Red DPHE dye solution in EtOH was added to 10 µl of this 1 mM aqueous solution of phospholipid (3 or POPC) and the mixture was briefly agitated. The corresponding mixture was finally monitored by fluorescence and phase contrast microscopy to determine the vesicle structure.

2.8. Transmission electron microscopy studies

2.8.1. General

A deposition system (Balzers Med010) was used to evaporate a homogeneous layer of carbon. The samples were collected over 400 mesh Cu grids. The grids were then negatively stained with a solution of 1% (w/w) uranyl acetate. Micrographs were recorded on an FEI Tecnai Sphera microscope operating at 200 kV and equipped with a LaB₆ electron gun, using the standard cryotransfer holders developed by Gatan, Inc. For image processing, micrographs were digitized in a Zeiss SCAI scanner with different sampling windows.

2.8.2. Transmission electron microscopy measurements

Copper grids (formvar/carbon-coated, 400 mesh copper) were prepared by glow discharging the surface at 20 mA for 1.5 min. Once the surface for vesicle adhesion was ready, 3.5 μ l of a 5 mM solution of phospholipid (3 or **POPC**) in H₂O (previously sonicated at \approx 55°C for 1 h) was deposited on the grid surface. This solution was allowed to sit for 10 s before being washed away with 10 drops of glass distilled H₂O and subsequent staining with 3 drops of 1% (w/w) uranyl acetate. The stain was allowed to sit for 10 s before wicking away with filter paper. All grid treatments and simple depositions were on the dark/shiny/glossy formvar-coated face of the grid (this side face up during glow discharge). Samples were then imaged via TEM, revealing the presence of several populations of spherical compartments (50–900 nm in diameter), consistent with a vesicle architecture.

2.9. Encapsulation experiments

2.9.1. Encapsulation of 8-hydroxypyrene-1,3,4-trisulfonic acid (standard method)

In total, 10 µl of a 10 mM solution of phospholipid (3 or POPC) in CHCl $_3$ was added to a 1 ml vial, placed under N_2 and dried for 15 min to prepare a lipid film. Then, 100 µl of 100 µM HPTS aqueous solution was added to the lipid film and briefly vortexed. The solution was tumbled at rt for 30 min. Afterwards, the resulting cloudy solution was diluted with an additional 200 µl of H_2O and transferred to a 100 kDa molecular weight cut-off (MWCO) centrifugal membrane filter and centrifuged for 3 min at 10 000 rcf (Eppendorf 5415C). The solution was similarly washed an additional five times to remove any nonencapsulated dye. Then, 5 µl of the vesicle solution was placed on a clean glass slide, secured by a greased coverslip and imaged on a spinning disc confocal microscope (488 nm laser) to observe encapsulation of HPTS.

2.9.2. Encapsulation of 8-hydroxypyrene-1,3,4-trisulfonic acid (inverse emulsion method)

In total, 60 µl of a 20 mM solution of phospholipid (3 or POPC) in CHCl3 was added to a 1 ml vial, placed under N2 and dried for 15 min to prepare a lipid film. Then, 200 µl of mineral oil was added and placed under N2 to displace the air above the mineral oil. The resulting mixture was sonicated with heat (≈55°C) for 1 h. Afterwards, 100 µl of the amidophospholipid oil was added to a 1 ml Eppendorf tube. Then, $10\,\mu l$ of the upper buffer (1 mM HPTS + 1 mM DTT + 50 mM NaCl + 200 mM sucrose in 100 mM HEPES buffer pH 7.5 solution) was added, and the resulting mixture was flicked and vortexed until it was a cloudy emulsion. The corresponding emulsion was added to a 1 ml Eppendorf tube containing 100 µl of the lower buffer (1 mM DTT + 50 mM NaCl + 200 mM glucose in 100 mM HEPES buffer pH 7.5 solution), so it floated on top. After waiting 10 min, the sample was centrifuged for 10 min at 9000–10 000 rcf. The sample was separated from the oil (either aspirating off the oil or using a syringe/needle to collect the sample from the bottom). The sample contained vesicles encapsulating HPTS which were then observed using fluorescence microscopy.

2.10. Anisotropy studies

2.10.1. Vesicle preparation and extrusion

In total, 50 μ l of a 20 mM solution of phospholipid (3 or POPC) in CHCl₃ was added to a 1 ml vial, placed under N₂ and dried for 15 min to prepare a lipid film. The dried film was hydrated in 500 μ l of H₂O (final concentration of phospholipid: 2 mM). The solution was briefly vortexed and then sonicated with heat (approx. 55°C) for 45 min. Once the sample was fully hydrated, it was extruded through a 100 nm membrane.

2.10.2. Anisotropy measurements

Downloaded from https://royalsocietypublishing.org/ on 15 September 2023

In total, 2 μl of a 500 μM solution of DPH in EtOH was added to 198 μl of 100 nm phospholipid (3 or POPC) extruded vesicles (final concentration of DPH: 5 μM , 1% v/v). The solution was tumbled at 25°C overnight. Steady-state anisotropy was measured at different temperatures (from -10 to 40°C) on a Perkin spectrophotometer with a manual polarizer accessory and Peltier temperature controller.

3. Results and discussion

3.1. Synthesis of amphiphilic precursors

We initially synthesized two substrates to mimic the native precursors of the common phospholipid POPC: an aminefunctionalized analogue of the lysophospholipid 1-palmitoylsn-glycerol-3-phosphocholine (1) (electronic supplementary material, scheme S1, figure S1) and an SNAC oleoyl thioester (2a) instead of oleoyl-CoA (electronic supplementary material, scheme S2, figure S1). It is worth noticing that 2a is slightly soluble in water, and the addition of organic solvents assures the complete solubilization of 2a and subsequent ligation. To facilitate direct aminolysis under exclusively aqueous conditions, we also synthesized a highly water-soluble thioester derivative, MESNA [33,34] oleoyl thioester (2b) (electronic supplementary material, scheme S2, figure S1) [13]. DLS experiments showed that precursor 2b formed micelles of approximately 2.8 nm in diameter (electronic supplementary material, figure S2) with CMCs below $10\,\mu\text{M}$ (electronic supplementary material, figure S3) [35].

3.2. Amidophospholipid 3 formation by directed aminolysis

We next explored the aminolysis reactions between the lysophospholipid 1 and the previously prepared oleoyl thioesters (2a,b) (figure 1). Amidophospholipid 3 formation was analysed over time using combined liquid chromatography (LC), mass spectrometry (MS) and evaporative light scattering detection (ELSD) measurements (electronic supplementary material, figure S1). Combination of the thioester (2a,b) and the lysophospholipid 1 in the appropriate conditions led to the production of 3 in aqueous conditions using millimolar concentrations of reactants (figure 1; electronic supplementary material, figure S1).

Synthesis of the amidophospholipid 3 by direct aminolysis between the amine-containing lysolipid 1 and the thioester 2a was initially studied. As expected, in the absence of any catalyst, phospholipid formation was not observed in organic polar solvents both at rt (table 1, entry 1; electronic supplementary material, table S1, entry 1) and 37°C (electronic supplementary material, table S1, entry 2). Ligations in organic/aqueous mixtures (table 1, entry 2; electronic supplementary material, table S1, entry 3) or water without organic solvents (table 1, entries 3 and 4) showed identical results.

Taking into consideration the slow rates of the aminolysis ligation, we next evaluated the generation of the phospholipid 3 in the presence of different additives. Metal ion-assisted aminolysis between 1 (30 mM) and 2a (30 mM) using CuBr₂ (30 mM) as additive in a mixture of CH₃CN/H₂O (1:1) led to the formation of the non-canonical phospholipid 3 in low conversion percentages (table 1, entries 5 and 6). Higher conversion rates were obtained by using AgNO₃ as additive (table 1, entries 7 and 8). Use of copper(I) species (electronic supplementary material, table S1, entry 4) did not produce the desired phospholipid, demonstrating that copper(II)based additives are more appropriate to accelerate aminolysis reactions. Phospholipid 3 synthesis was also not detected upon addition of divalent metal ions other than copper(II) (electronic supplementary material, table S1, entries 5-7) or gold species (electronic supplementary material, table S1, entries 8 and 9). Interestingly, decreased levels of phospholipid conversion were observed by using metal ion-assisted aminolysis approaches in water without organic solvent (table 1, entries 9-12). We believe that this effect is likely due to the low water solubility of the thioester 2a.

Alternatively, imidazole-promoted aminolysis between lysolipid 1 and thioester 2a resulted in higher conversion rates (table 1, entries 13–16), leading to good yields (81%) after 20 h at 37°C (table 1, entry 16).

To avoid the use of organic solvents and solubility issues related with the derivative **2a**, we next evaluated the aminolysis reaction between the lysophospholipid **1** and the water-soluble thioester **2b**. Preliminary experiments demonstrated that phospholipid **3** formation did not take place in the absence of additives (table 1, entries 17 and 18; electronic supplementary material, table S1, entries 10–13). Metal ion-assisted aminolysis afforded phospholipid **3** in low conversion percentages (table 1, entries 19 and 20) when CuBr₂ was used. Better results were obtained when AgNO₃ was employed (table 1, entries 21 and 22), observing conversion percentages higher than 50% (table 1, entry 22). Surprisingly, utilization of different silver(I) species rather than AgNO₃ did

Table 1. Optimization of the direct aminolysis conditions for the synthesis of the amidophospholipid 3.

entry	aminolysis ^a	thioester ^b	additive	solvent	T (°C)	<i>T</i> (h)	3 (%)
1		2a		CH ₃ CN	rt ^c	20	nd ^d
2		2a		CH ₃ CN/H ₂ O (1:1)	rt	20	nd
3		2a		H_2O	rt	20	nd
4		2a		H_2O	rt	37	nd
5	MIA	2a	CuBr ₂ (30 mM)	CH ₃ CN/H ₂ O (1:1)	rt	20	4
6	MIA	2a	CuBr ₂ (30 mM)	CH ₃ CN/H ₂ O (1:1)	37	20	11
7	MIA	2a	$AgNO_3$ (30 mM)	CH ₃ CN/H ₂ O (1:1)	rt	20	23
8	MIA	2a	$AgNO_3$ (30 mM)	CH ₃ CN/H ₂ O (1:1)	37	20	48
9	MIA	2a	CuBr ₂ (30 mM)	H_2O	rt	20	nd
10	MIA	2a	CuBr ₂ (30 mM)	H_2O	37	20	3
11	MIA	2a	$AgNO_3$ (30 mM)	H_2O	rt	20	6
12	MIA	2a	$AgNO_3$ (30 mM)	H_2O	37	20	21
13	IP	2a	lm (1.5 M)	H_2O	rt	2	3
14	IP	2a	lm (1.5 M)	H_2O	rt	20	65
15	IP	2a	lm (1.5 M)	H_2O	37	2	8
16	IP	2a	lm (1.5 M)	H_2O	37	20	81
17		2b		H_2O	rt	20	nd
18		2b		H_2O	37	20	nd
19	MIA	2b	CuBr ₂ (30 mM)	H_2O	rt	20	6
20	MIA	2b	CuBr ₂ (30 mM)	H_2O	37	20	14
21	MIA	2b	$AgNO_3$ (30 mM)	H_2O	rt	20	29
22	MIA	2b	$AgNO_3$ (30 mM)	H_2O	37	20	53
23	IP	2b	lm (1.5 M)	H_2O	rt	2	88
24	IP	2b	lm (1.5 M)	H_2O	rt	20	99
25	IP	2b	lm (1.5 M)	H_2O	37	1	96
26	IP	2b	lm (1.5 M)	H_2O	37	2	99
27	IP	2b	lm (1.5 M)	H_2O	37	20	99
28	IP	2b	Boc-His-OH (1.5 M)	H_2O	37	20	3
29	IP	2b	2- ^{Me} lm (1.5 M)	H_2O	37	2	46
30	IP	2b	2- ^{Me} lm (1.5 M)	H₂0	37	20	81
31	IP	2b	2- ^{Et} lm (1.5 M)	H₂0	37	2	nd
32	IP	2b	2- ^{Et} lm (1.5 M)	H₂0	37	20	2
33	IP	2b	2- ^{Un} lm (1.5 M)	H₂0	37	2	3
34	IP	2b	2- ^{Un} lm (1.5 M)	H ₂ O	37	20	4

^aMetal ion-assisted (MIA) or imidazole-promoted (IP) aminolysis.

not enable the generation of the desired phospholipid (electronic supplementary material, table S1, entries 14 and 15).

Imidazole-promoted aminolysis between 1 and 2b resulted in higher conversion rates (table 1, entries 23–27) compared to the metal ion-assisted reactions. In the presence of imidazole, the addition of the thioester 2b to the amine-containing lysophospholipid 1 immediately led to amidophospholipid 3 formation, and this process progressed to near completion after approximately 2 h using millimolar concentrations of reactants (figure 2; electronic supplementary material,

figure S1). Interestingly, ligations in organic (electronic supplementary material, table S1, entry 16) or organic/aqueous mixtures (electronic supplementary material, table S1, entry 17) showed minimal phospholipid production. This is likely a consequence of the poor solubility of thioester **2b** in such organic solvents, thus hindering the ligation process.

Phospholipid 3 formation was only minimally observed when using Boc-His-OH, a relevant imidazole-containing amino acid derivative (table 1, entry 28; electronic supplementary material, table S1, entry 18). Taking this into

^bThioester (**2a,b**) concentration: 30 mM. Ratio 1:1 with the lysolipid **1** (30 mM).

^cRoom temperature (approx. 25°C).

^dNot detected (nd).

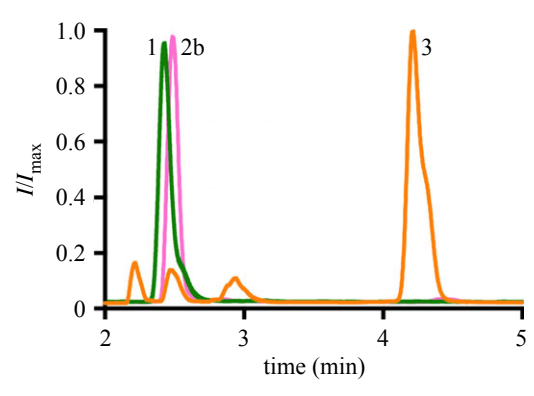


Figure 2. Monitoring amidophospholipid formation by HPLC/ELSD/MS. ELSD traces corresponding to the purified lysophospholipid 1, MESNA oleoyl thioester 2b, and amidophospholipid 3. The retention times were verified by mass spectrometry and the use of known standards.

consideration, we next studied the effect of the imidazole substitution on the aminolysis reaction. Interestingly, ligations in the presence of a monomethylated imidazole (2-MeIm) afforded phospholipid 3 conversion percentages from moderate (table 1, entry 29) to good (table 1, entry 30) yield depending on the analysed time scale. Alternatively, use of ethyl- (table 1, entries 31 and 32) or undecyl-based imidazoles (table 1, entries 33 and 34) resulted in much lower phospholipid conversions, probably as a consequence of a significant steric hindrance effect during the ligation process. These studies clearly demonstrated that non-substituted imidazole affords the highest conversion rates for the formation of the non-canonical amidophospholipid 3 via direct aminolysis in aqueous solution.

3.3. Anisotropy studies: determination of chain-melting temperatures in amidophospholipid 3

Downloaded from https://royalsocietypublishing.org/ on 15 September 2023

We next determined the chain-melting temperature of the purified phospholipid 3 (figure 3). In particular, 1,6-diphenyl-1,3,5-hexatriene (DPH) anisotropy as a function of temperature was used to estimate the phase transition of the lipid chains [36]. A sudden change in the slope of the anisotropy indicates a transition from gel to liquid-crystalline phase (figure 3). The melting temperature of the lipid chains in 3 membranes was detected at 276 K. The measurements indicate that the amidophospholipid 3 membranes are well ordered, with fluidity and chain-melting temperatures comparable to those of native POPC membranes (T_C = 270 K) [37].

3.4. Characterization of the amidophospholipid 3 vesicular structures

We next performed microscopy studies to characterize the self-assembled lipid structures. As expected, neither the amine-modified lysophospholipid 1 nor the MESNA oleoyl thioester 2b formed membranes in aqueous solution. However, the purified amidophospholipid 3, when hydrated, readily formed membrane-bound vesicles. Lipid vesicular structures were initially identified by phase-contrast microscopy (figure 4a) and fluorescence microscopy using the membrane-staining dye Texas Red® DHPE (figure 4b). TEM also corroborated the formation of vesicular structures (figure 4c; electronic supplementary material, figure S4a).

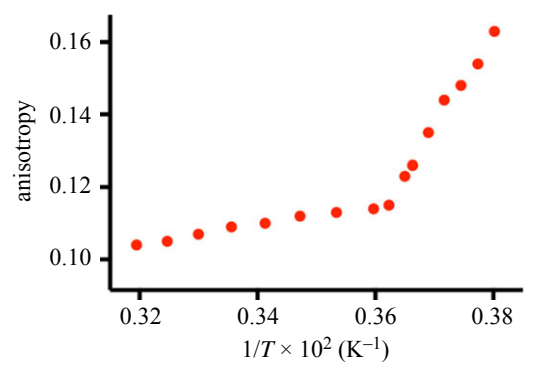


Figure 3. DPH anisotropy graph corresponding to a sample of phospholipid 3 vesicles. The melting temperature of the lipid chains in phospholipid 3 membranes was detected at 276 K.

Additionally, amidophospholipid 3 vesicles were able to efficiently encapsulate polar fluorophore dyes, such as HPTS (figure 4d).

3.5. POPC formation by directed esterification

Having shown that metal- and imidazole-promoted reactions enable the construction of biomimetic phospholipids by direct aminolysis ligations, we next evaluated if esterification ligations were feasible. Esterification between lysophospholipids and acyl thioesters would afford native phospholipids. Living organisms synthesize phospholipids through enzymatic acylation of lysophospholipids [38,39]. Nonetheless, enzymefree esterification methods to form natural phospholipids in aqueous conditions remain both challenging and limited in scope [40,41]. Recent studies have shown successful monoacylation of lysophospholipids under alkaline conditions [42]. Considering the importance of developing a high-yielding synthesis of natural phospholipids in water [43], we explored the direct esterification between the lysophospholipid 1-palmitoyl-2-hydroxy-sn-glycero-3-phosphocholine (Lyso C₁₈ PC) and the previously prepared oleoyl thioesters (2a,b) (figure 5). POPC synthesis was analysed over time using HPLC-ELSD-MS (electronic supplementary material, figure S1). The addition of the thioester (2a,b) to the lysophospholipid Lyso C₁₆ PC in the appropriate conditions led to POPC formation in aqueous conditions using millimolar concentrations of reactants (figure 5; electronic supplementary material, figure S1).

We initially analysed the formation of POPC by direct esterification between Lyso C₁₆ PC and the thioester 2a. As expected, in the absence of any catalyst, phospholipid formation was not observed (table 2, entries 1 and 2; electronic supplementary material, table S2, entry 1). Surprisingly, addition of metals or imidazole did not enable an efficient synthesis of the corresponding natural phospholipid (table 2, entries 3–5; electronic supplementary material, table S2, entries 2 and 3), highlighting the complexity of such esterification reactions in aqueous conditions.

Expecting an improved reactivity by using more water-soluble precursors, we next studied the esterification reaction between Lyso C₁₆ PC and the thioester 2b. Initial experiments showed no formation of POPC in the absence of catalysts (table 2, entries 6 and 7). Metal ion-assisted esterifications led to the formation of the natural phospholipid in very low conversions (table 2, entries 8 and 9). Alternatively, imidazolepromoted esterifications resulted in higher conversion rates

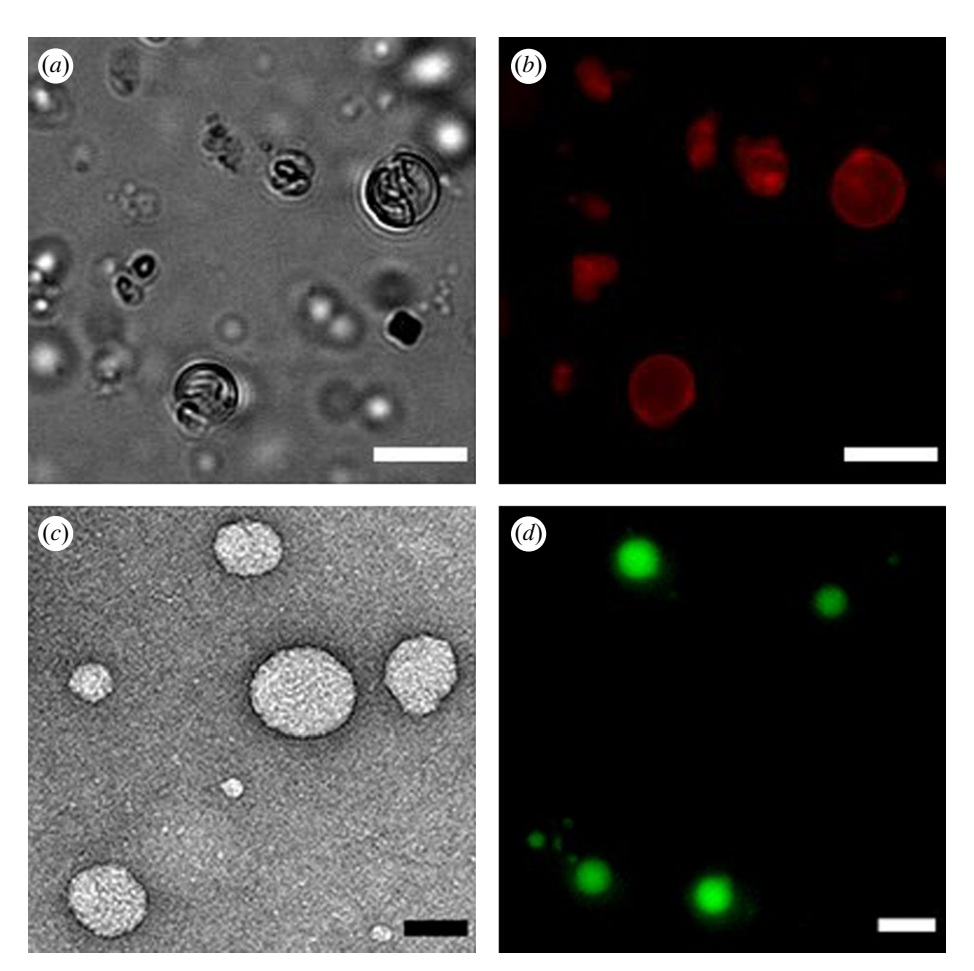


Figure 4. Characterization of the amidophospholipid vesicular structures. (*a*) Phase-contrast microscopy image of membrane vesicles resulting from the self-assembly of **3.** Scale bar denotes 5 μm. (*b*) Fluorescence microscopy image of vesicles formed by hydration of a thin film of **3.** Membranes were stained using 0.1 mol% Texas Red DHPE. Scale bar denotes 5 μm. (*c*) TEM image of negatively stained amidophospholipid **3** vesicles. Scale bar denotes 50 nm. (*d*) Fluorescence image demonstrating the encapsulation of HPTS in membrane vesicles of **3.** Scale bar denotes 5 μm.

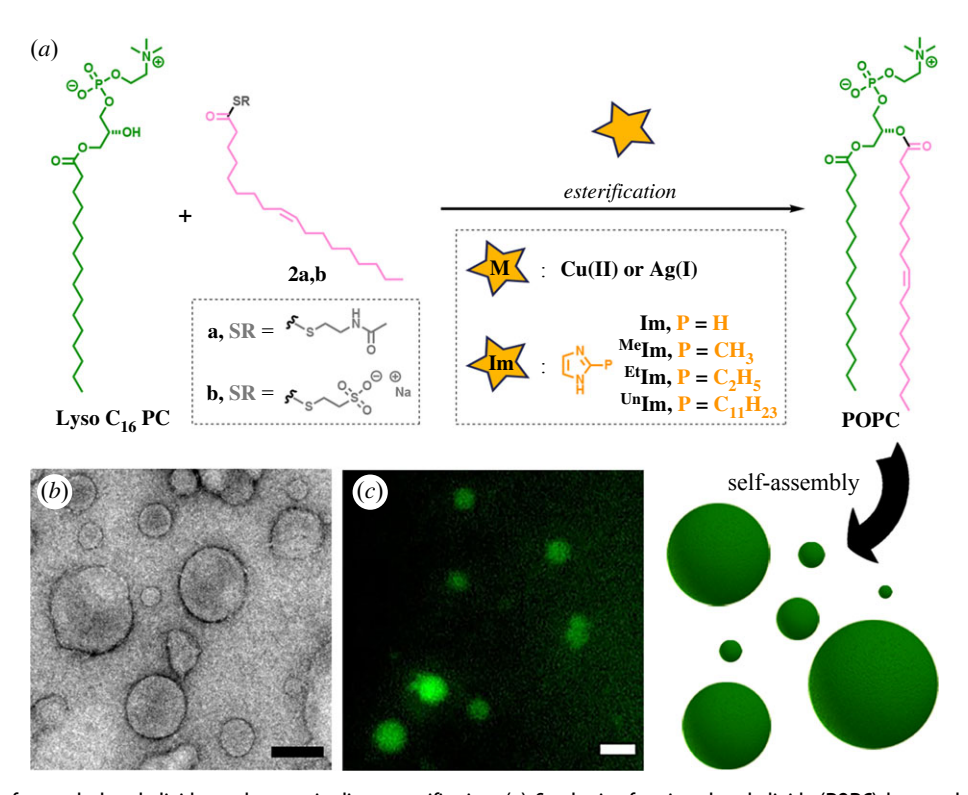


Figure 5. Construction of natural phospholipid membranes via direct esterification. (*a*) Synthesis of native phospholipids (**POPC**) by metal- or imidazole-promoted esterification ligations between a lysophospholipid (**Lyso C**₁₆ **PC**) and an oleoyl thioester (**2a,b**). The corresponding lipid self-assembles into vesicular structures. (*b*) TEM image of negatively stained **POPC** liposomes. Scale bar denotes 100 nm. (*c*) Fluorescence image demonstrating the encapsulation of HPTS in **POPC** vesicles. Scale bar denotes 25 µm. Purified **POPC** employed for (*b,c*) was obtained via either metal ion-assisted or imidazole-promoted esterification.

Table 2. Optimization of the esterification conditions for the synthesis of POPC.

entry	esterification ^a	thioester ^b	additive	solvent	<i>T</i> (°C)	<i>T</i> (h)	POPC (%)
1		2a		CH ₃ CN/H ₂ O (1:1)	rt ^c	20	nd ^d
2		2a		CH ₃ CN/H ₂ O (1:1)	37	20	nd
3	MIA	2a	CuBr ₂ (30 mM)	CH ₃ CN/H ₂ O (1:1)	rt	20	2
4	MIA	2a	AgNO ₃ (30 mM)	CH ₃ CN/H ₂ O (1:1)	rt	20	3
5	IP	2a	lm (1.5 M)	H ₂ O	rt	20	5
6		2b		H ₂ O	rt	20	nd
7		2b		H ₂ O	37	20	nd
8	MIA	2b	CuBr ₂ (30 mM)	H ₂ 0	rt	20	3
9	MIA	2b	AgNO ₃ (30 mM)	H ₂ O	rt	20	4
10	IP	2b	lm (1.5 M)	H ₂ O	rt	2	6
11	IP	2b	lm (1.5 M)	H ₂ O	rt	20	21
12	IP	2b	lm (1.5 M)	H ₂ O	37	2	15
13	IP	2b	lm (1.5 M)	H ₂ O	37	20	54
14	IP	2b	Im (1.5 M) + CuBr ₂ (30 mM)	H ₂ 0	37	2	9
15	IP	2b	Im (1.5 M) + AgNO ₃ (30 mM)	H ₂ O	37	2	15
16	IP	2b	1- ^{Me} lm (1.5 M)	H ₂ 0	rt	20	nd
17	IP	2b	1- ^{Me} lm (1.5 M)	H ₂ O	37	20	5
18	IP	2b	2- ^{Me} lm (1.5 M)	H ₂ O	rt	20	5
19	IP	2b	2- ^{Me} lm (1.5 M)	H ₂ 0	37	20	7
20	IP	2b	4(5)- ^{Me} lm (1.5 M)	H ₂ 0	rt	20	9
21	IP	2b	4(5)- ^{Me} lm (1.5 M)	H ₂ 0	37	20	12
22	IP	2b	2- ^{Et} lm (1.5 M)	H ₂ O	rt	20	4
23	IP	2b	2- ^{Et} lm (1.5 M)	H ₂ O	37	20	5
24	IP	2b	2- ^{Un} lm (1.5 M)	H ₂ O	rt	20	3
25	IP	2b	2- ^{Un} lm (1.5 M)	H ₂ O	37	20	4
26	IP	2b	2- ^{Et} -4- ^{Me} lm (1.5 M)	H₂0	rt	20	2
27	IP	2b	2- ^{Et} -4- ^{Me} lm (1.5 M)	H ₂ O	37	20	3

^aMetal ion-assisted (MIA) or imidazole-promoted (IP) esterification.

(table 2, entries 10–13), with the best conditions leading to moderate conversion (54%) after 20 h at 37°C (table 2, entry 13). While modest, these ligation yields are promising, especially if we consider that these reactions result in the synthesis of natural phospholipids in aqueous solution by a one-pot enzyme-free esterification method. Addition of metals to the imidazole medium did not lead to an increase in the conversion rates of the esterification reaction (table 2, entries 14 and 15).

Interestingly, POPC formation was not observed using biologically relevant imidazole-containing molecules, such as histidine or histamine (electronic supplementary material, table S2, entries 4–9). We thus believe that the imidazole substitution and its hydrophobic character significantly affect the phospholipid ligation. Taking this into consideration, we evaluated the formation of POPC by direct esterification reactions in the presence of different alkylimidazoles (table 2, entries 16–27). In the case of monomethylated imidazoles, we observed that derivatives with a methyl group in the position

4(5) (table 2, entries 20 and 21) led to higher **POPC** conversions than imidazoles with methyl substitutions in the positions 1 (table 2, entries 16 and 17) or 2 (table 2, entries 18 and 19). Regarding the hydrophobic character, we observed that incorporation of larger alkyl substitutions (i.e. ethyl, undecyl) (table 2, entries 22–25) resulted in lower conversions, likely due a steric effect during the ligation process. Double-substituted imidazoles also resulted in very low conversions (table 2, entries 26 and 27), probably due to a similar effect. These results showed that non-substituted imidazole offers the highest conversion rates for the synthesis of natural **POPC**.

3.6. Anisotropy studies: determination of chain-melting temperatures in **POPC**

DPH anisotropy measurements on purified **POPC** samples obtained via either metal ion-assisted or imidazole-promoted esterification showed that the melting temperature of the lipid chains was 270 K, which corresponds to the values

^bThioester (**2a,b**) concentration: 30 mM. Ratio 1:1 with the **Lyso C₁₆ PC** (30 mM).

^cRoom temperature (approx. 25°C).

dNot detected (nd).

previously reported in the literature for POPC membranes (electronic supplementary material, figure S5) [37].

3.7. Characterization of the **POPC** vesicular structures

A thin film of the purified POPC, when hydrated, readily formed micrometre-sized vesicles (figure 5; electronic supplementary material, figure S6). Vesicular assemblies were identified by phase-contrast microscopy (electronic supplementary material, figure S6a) and fluorescence microscopy using Texas Red DHPE (electronic supplementary material, figure S6b). Confirmation that the resulting structures were membrane compartments was also achieved by negative staining TEM (figure 5b; electronic supplementary material, figure S4b). We also demonstrated that the corresponding liposomes were capable of encapsulating HPTS (figure 5c).

4. Conclusion

Here we report that direct aminolysis ligations allow the preparation of a new class of amidophospholipids, which spontaneously self-assemble to form vesicular structures. Thus, aminolysis reactions can be efficiently used as a nonenzymatic methodology to drive the de novo self-assembly of amidophospholipid membranes. Such biomimetic membranes could be employed in applications involving synthetic cells, as well as in the construction of drug-delivery systems and microreactors. Additionally, we have explored the suitability of the non-enzymatic approaches for driving the in situ formation of native phospholipid membranes via direct esterification. These studies could bring new insights into the origin of cellular membranes and open up multiple avenues for the straightforward non-enzymatic synthesis of membrane-forming phospholipids for artificial cells.

Data accessibility. The data are provided in electronic supplementary material [44].

Authors' contributions. F.A.S.-T.: data curation, formal analysis, investigation, methodology, validation, visualization, writing-review and editing; R.J.B.: conceptualization, data curation, formal analysis, funding acquisition, investigation, methodology, project administration, resources, supervision, validation, visualization, writingoriginal draft, writing-review and editing; N.K.D.: conceptualization, funding acquisition, project administration, resources, supervision, writing-review and editing.

All authors gave final approval for publication and agreed to be held accountable for the work performed therein.

Conflict of interest declaration. The authors declare no competing interests. Funding. This work was supported by the Agencia Estatal de Investigación (AEI) and the Ministerio de Ciencia e Innovación (MICINN) [PID2021-128113NA-I00], the National Science Foundation (NSF) [MCB-2124105] and the National Institutes of Health (NIH) [R35GM141939]. R.J.B. also thanks the Agencia Estatal de Investigación (AEI) and the Ministerio de Ciencia e Innovación (MICINN) for his Ramón y Cajal contract (RYC2020-030065-I).

References

Downloaded from https://royalsocietypublishing.org/ on 15 September 2023

- Bhattacharya A, Brea RJ, Devaraj NK. 2017 De novo vesicle formation and growth: an integrative approach to artificial cells. Chem. Sci. 8, 7912-7922. (doi:10.1039/C7SC02339A)
- Brea RJ, Hardy MD, Devaraj NK. 2015 Towards selfassembled hybrid artificial cells: novel bottom-up approaches to functional synthetic membranes. Chem. Eur. J. 21, 12 564-12 570. (doi:10.1002/ CHEM.201501229)
- 3. Buddingh' BC, Van Hest JCM. 2017 Artificial cells: synthetic compartments with life-like functionality and adaptivity. Acc. Chem. Res. 50, 769-777. (doi:10.1021/acs.accounts.6b00512)
- Devaraj NK. 2017 In situ synthesis of phospholipid membranes. J. Org. Chem. 82, 5997-6005. (doi:10. 1021/acs.joc.7b00604)
- Dawson PE, Muir TW, Clark-Lewis I, Kent SBH. 1994 Synthesis of proteins by native chemical ligation. Science 266, 776-779. (doi:10.1126/science. 7973629)
- Wieland T, Bokelmann E, Bauer L, Lang HU, Lau H. 1953 Über Peptidsynthesen. 8. Mitteilung. Bildung von S-haltigen Peptiden durch intramolekulare Wanderung von Aminoacylresten. Liebigs Ann. Chem. 583, 129-149. (doi:10.1002/jlac. 19535830110)
- 7. Vázquez O, Seitz O. 2014 Templated native chemical ligation: peptide chemistry beyond protein synthesis. J. Pept. Sci. 20, 78-86. (doi:10.1002/psc. 2602)

- Raibaut L, Ollivier N, Melnyk O. 2012 Sequential native peptide ligation strategies for total chemical protein synthesis. Chem. Soc. Rev. 41, 7001-7015. (doi:10.1039/C2CS35147A)
- Hackenberger CPR, Schwarzer D. 2008 Chemoselective ligation and modification strategies for peptides and proteins. Angew. Chem. Int. Ed. 47, 10 030-10 074. (doi:10.1002/anie.200801313)
- 10. Brea RJ, Cole CM, Lyda BR, Ye L, Prosser RS, Sunahara RK, Devaraj NK. 2017 In situ reconstitution of the adenosine A2A receptor in spontaneously formed synthetic liposomes. J. Am. Chem. Soc. 139, 3607-3610. (doi:10.1021/jacs.6b12830)
- 11. Brea RJ, Rudd AK, Devaraj NK. 2016 Nonenzymatic biomimetic remodeling of phospholipids in synthetic liposomes. Proc. Natl Acad. Sci. USA 113, 8589-8594. (doi:10.1073/pnas.1605541113)
- 12. Cole CM, Brea RJ, Kim YH, Hardy MD, Yang J, Devaraj NK. 2015 Spontaneous reconstitution of functional transmembrane proteins during bioorthogonal phospholipid membrane synthesis. Angew. Chem. Int. Ed. 54, 12 738-12 742. (doi:10. 1002/anie.201504339)
- 13. Brea RJ, Cole CM, Devaraj NK. 2014 In situ vesicle formation by native chemical ligation. Angew. Chem. Int. Ed. 53, 14 102-14 105. (doi:10.1002/ anie.201408538)
- 14. Bhattacharya A, Brea RJ, Niederholtmeyer H, Devaraj NK. 2019 A minimal biochemical route towards de novo formation of synthetic phospholipid

- membranes. Nat. Commun. 10, 300. (doi:10.1038/ s41467-018-08174-x)
- 15. Enomoto T, Brea RJ, Bhattacharya A, Devaraj NK. 2018 In situ lipid membrane formation triggered by intramolecular photoinduced electron transfer. Langmuir 34, 750-755. (doi:10.1021/acs.langmuir. 7b02783)
- 16. Seoane A, Brea RJ, Fuertes A, Podolsky KA, Devaraj NK. 2018 Biomimetic generation and remodeling of phospholipid membranes by dynamic imine chemistry. J. Am. Chem. Soc. 140, 8388-8391. (doi:10.1021/jacs.8b04557)
- 17. Brea RJ, Bhattacharya A, Devaraj NK. 2017 Spontaneous phospholipid membrane formation by histidine ligation. Synlett 28, 108-112. (doi:10. 1055/s-0036-1588634)
- 18. Budin I, Devaraj NK. 2012 Membrane assembly driven by a biomimetic coupling reaction. J. Am. Chem. Soc. 134, 751-753. (doi:10.1021/ja2076873)
- 19. Payne RJ, Wong CH. 2010 Advances in chemical ligation strategies for the synthesis of glycopeptides and glycoproteins. Chem. Commun. 46, 21-43. (doi:10.1039/B913845E)
- 20. Payne RJ, Ficht S, Greenberg WA, Wong CH. 2008 Cysteine-free peptide and glycopeptide ligation by direct aminolysis. Angew. Chem. Int. Ed. 47, 4411-4415. (doi:10.1002/anie.200705298)
- 21. Du JJ, Xin LM, Lei Z, Zou SY, Xu WB, Wang CW, Zhang L, Gao XF, Guo J. 2018 Glycopeptide ligation via direct aminolysis of selenoester. Chin. Chem.

- Lett. 29, 1127-1130. (doi:10.1016/j.cclet.2018.04. 016
- 22. Du JJ, Zhang L, Gao XF, Sun H, Guo J. 2020 Peptidyl ω-Asp selenoesters enable efficient synthesis of Nlinked glycopeptides. Front. Chem. 8, 396. (doi:10. 3389/fchem.2020.00396)
- 23. Yang J, Zhao J. 2017 Recent developments in peptide ligation independent of amino acid sidechain functional group. Sci. China Chem. 61, 97-112. (doi:10.1007/s11426-017-9056-5)
- 24. Agrigento P, Albericio F, Chamoin S, Dacquignies I, Koc H, Eberle M. 2014 Facile and mild synthesis of linear and cyclic peptides via thioesters. Org. Lett. 16, 3922-3925. (doi:10.1021/ol501669n)
- 25. Burke HM, McSweeney L, Scanlan EM. 2017 Exploring chemoselective S-to-N acyl transfer reactions in synthesis and chemical biology. Nat. Commun. 8, 15655. (doi:10.1038/ncomms15655)
- 26. Kawakami T, Yoshimura S, Aimoto S. 1998 Synthesis of reaper, a cysteine-containing polypeptide, using a peptide thioester in the presence of silver chloride as an activator. Tetrahedron Lett. 39, 7901-7904. (doi:10.1016/S0040-4039(98)01752-3)
- 27. Teruya K, Kawakami T, Akaji K, Aimoto S. 2002 Total synthesis of [L40I, C90A, C109A]-human T-cell leukemia virus type 1 protease. Tetrahedron Lett. 43, 1487-1490. (doi:10.1016/S0040-4039(02)00040-0)
- Chen G, Wan Q, Tan Z, Kan C, Hua Z, Ranganathan K, Danishefsky SJ. 2007 Development of efficient methods for accomplishing cysteine-free peptide and glycopeptide coupling. Angew. Chem. Int. Ed. 46, 7383-7387. (doi:10.1002/anie. 200702865)

Downloaded from https://royalsocietypublishing.org/ on 15 September 2023

29. Zhang L, Tam JP. 1999 Lactone and lactam library synthesis by silver ion-assisted orthogonal

- cyclization of unprotected peptides. J. Am. Chem. Soc. 121, 3311-3320. (doi:10.1021/ja983859d)
- 30. Li Y, Yongye A, Giulianotti M, Martinez-Mayorga K, Yu Y, Houghten RA. 2009 Synthesis of cyclic peptides through direct aminolysis of peptide thioesters catalyzed by imidazole in aqueous organic solutions. J. Comb. Chem. 11, 1066-1072. (doi:10.1021/cc900100z)
- 31. Li Y, Giulionatti M, Houghten RA. 2010 Macrolactonization of peptide thioesters catalyzed by imidazole and its application in the synthesis of kahalalide B and analogues. Org. Lett. 12, 2250-2253. (doi:10.1021/ol100596p)
- 32. Yamada H, Kuroki R, Hirata M, Imoto T. 1983 Intramolecular cross-linkage of lysozyme. Imidazole catalysis of the formation of the cross-link between lysine-13 (ε -amino) and leucine-129 (α -carboxyl) by carbodiimide reaction. Biochemistry 22, 4551-4556. (doi:10.1021/bi00288a031)
- 33. Mashiach E, Sela S, Weinstein T, Cohen HI, Shasha SM, Kristal B. 2001 Mesna: a novel renoprotective antioxidant in ischaemic acute renal failure. Nephrol. Dial. Transplant. 16, 542-551. (doi:10.1093/ndt/16. 3.542)
- 34. Rise F, Undheim K. 1989 Sodium 2mercaptoethanesulfonate in reversible adduct formation and water solubilization. Acta Chem. Scand. 43, 489-492. (doi:10.3891/acta.chem.scand.
- 35. Stafford RE, Fanni T, Dennis EA. 1989 Interfacial properties and critical micelle concentration of lysophospholipids. Biochemistry 28, 5113-5120. (doi:10.1021/bi00438a031)
- Lentz BR, Barenholz Y, Thompson TE. 1976 Fluorescence depolarization studies of phase transitions and fluidity in phospholipid

- bilayers. 1. Single component phosphatidylcholine liposomes. Biochemistry 15, 4521-4528. (doi:10. 1021/bi00665a029)
- 37. Litman BJ, Neil Lewis E, Levin IW. 1991 Packing characteristics of highly unsaturated bilayer lipids: Raman spectroscopic studies of multilamellar phosphatidylcholine dispersions. Biochemistry 30, 313-319. (doi:10.1021/bi00216a001)
- 38. Shindou H, Hishikawa D, Harayama T, Yuki K, Shimizu T. 2009 Recent progress on acyl CoA: lysophospholipid acyltransferase research. J. Lipid Res. 50, S46-S51. (doi:10.1194/jlr.R800035-JLR200)
- Shindou H, Shimizu T. 2009 Acyl-CoA: lysophospholipid acyltransferases. J. Biol. Chem. 284, 1-5. (doi:10.1074/jbc.R800046200)
- 40. Fernández-García C, Powner MW. 2017 Selective acylation of nucleosides, nucleotides, and glycerol-3-phosphocholine in water. Synlett 28, 78-83. (doi:10.1055/s-0036-1588626)
- 41. Bonfio C, Caumes C, Duffy CD, Patel BH, Percivalle C, Tsanakopoulou M, Sutherland JD. 2019 Lengthselective synthesis of acylglycerol-phosphates through energy-dissipative cycling. J. Am. Chem. Soc. 141, 3934-3939. (doi:10.1021/jacs.8b12331)
- 42. Liu L, Zou Y, Bhattacharya A, Zhang D, Lang SQ, Houk KN, Devaraj NK. 2020 Enzyme-free synthesis of natural phospholipids in water. Nat. Chem. 12, 1029-1034. (doi:10.1038/s41557-020-00559-0)
- 43. Testet E, Akermoun M, Shimoji M, Cassagne C, Bessoule JJ. 2002 Nonenzymatic synthesis of glycerolipids catalyzed by imidazole. J. Lipid Res. 43, 1150-1154. (doi:10.1194/jlr.M200075-JLR200)
- 44. Souto-Trinei FA, Brea RJ, Devaraj NK. 2023 Biomimetic construction of phospholipid membranes by direct aminolysis ligations. Figshare. (doi:10.6084/m9.figshare.c.6673513)